Low-Energy Nuclear Physics: Problems and Solutions

Amur Margaryan
Alikhanyan National Science Laboratory

Ultrafast Beams and Applications 2-5 July 2019 Yerevan

Outline

- **Ultrafast Beams and Applications in Nuclear Physics**

What we have at CANDLE, and how it can be used for Nuclear Physics

- **Decay pion spectroscopy of Λ-hypernuclei**
- **Auger Neutron Spectroscopy of Λ-hypernuclei**
- **Heavy Shape Isomer Spectroscopy**
- **RF-Timing Technique**
- **Cluster Structure of Nuclei**
- **Low-Energy Nuclear Astrophysics**
- **Low Energy Nuclear Interaction Chamber**
- **Conclusions**

Ultrafast Beams and Applications in Nuclear Physics

RF driven electron accelerators provide ultrafast, picosecond duration, CW high-energy electron-photon beams for nuclear studies (MAMI, JLAB, etc)

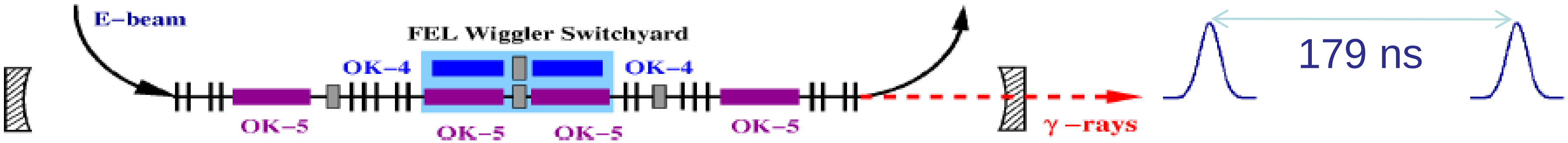

Diagram of HIγS high-flux, quasi-CW, 5.5796 MHz γ-ray beam time.
Typical collimated flux ($\Delta E\gamma / E\gamma$ = 5% FWHM) = 2.4×10^8 photon/s at $E\gamma \leq 11$ MeV
Photon beam bunch-length ≤ 200 ps, distance between bunches = 179 ns.
Number of photons/bunch = 43

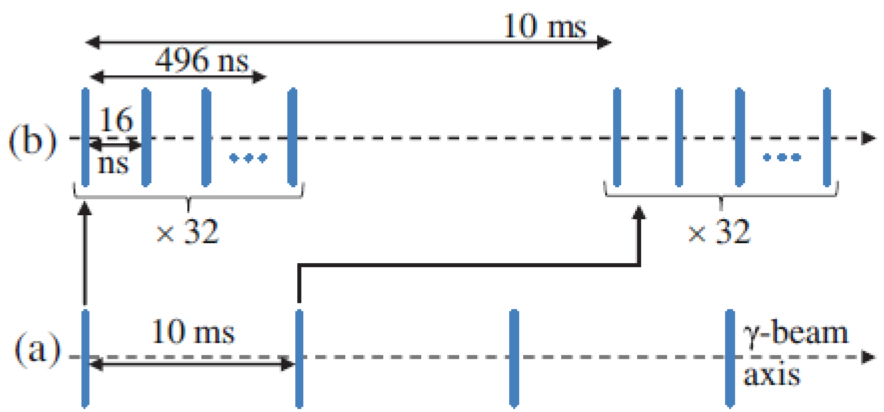

Expected collimated flux ($\Delta E\gamma / E\gamma$ = 0.5% FWHM) = 8.3×10^8 photon/s at $E\gamma \leq 19$ MeV
Photon bunch-length ≤ 1ps
Number of photons/bunch =2.6×10^5

Diagram of ELI-NP γ-ray beam time structure where (a) represents the 100Hz macro-structure and (b) the γ-ray beam micro-structure.

Advanced Research Electron Accelerator Laboratory

RF Synchronized Photon Electron Beams

Photon Beams

- Wavelength – 1030 nm; 515 nm; 259 nm
- Pulse Repetition rate-50 MHz; 1 Hz-100 kHz
- Bunch Length – 0.4ps – 10ps

Electron Beams

- Energy (max) – 4.7 MeV
- Charge (max) – 10-250 pC
- Bunch Length – 0.4ps – 10ps
- Energy spread – 1.5 %
- Pulse Repetition rate – 1-20 Hz

Discovery of Λ hypernucleus
Marian Danysz and Jerzy Pniewski, 1952

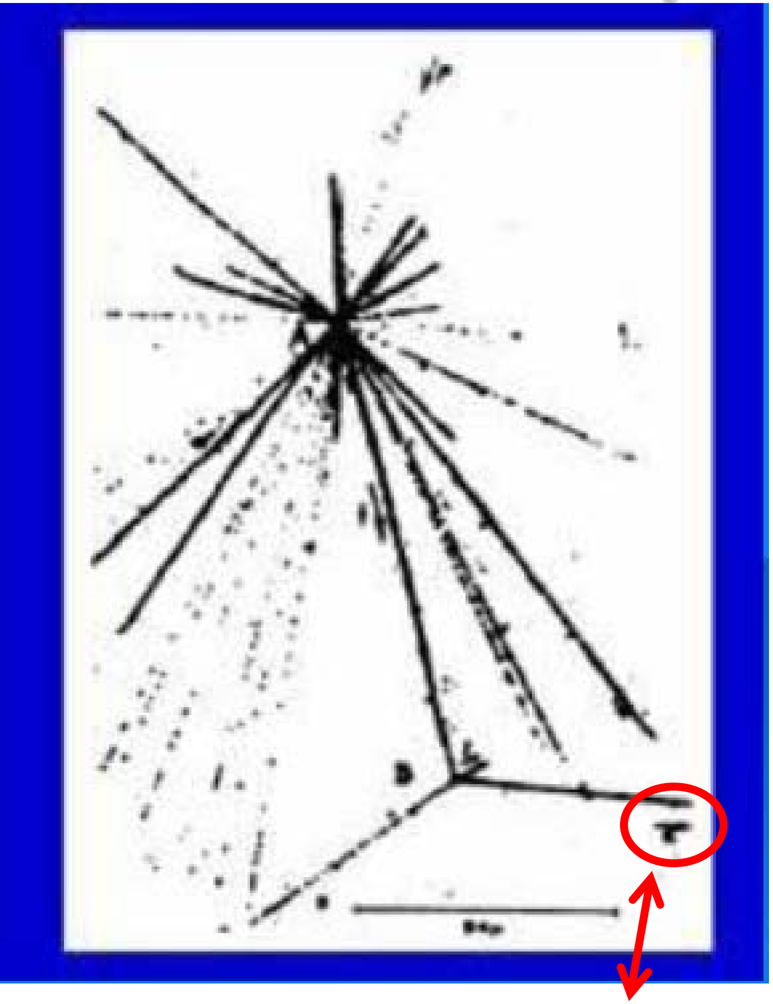

- Pionic decay
- Hyperfragments/stars < 0.001
- Delayed pionic decay
- Extensive studies at sixties of last century mainly used to determine the binding energy of light (A≤15) hypernuclei in emulsion
- Precision: ~50keV
- Resolution: ~0.5 – 1.0 MeV
- Problems:

  - Poor statistics

  - Calibrations (poor accuracy)

Hyperfragment π^- delayed decay (${}_{\Lambda}^{4}H \longrightarrow {}^{4}He + \pi^-$)

Nuclei ⟵ Baryon-Baryon Interaction ⟶ Neutron Star

~42-known, 24 as a hyperfragment
Expected number > 8000

Ambartsumyan and Saakyan 1960

Regular nuclei~3000 - known
Expected ~8000

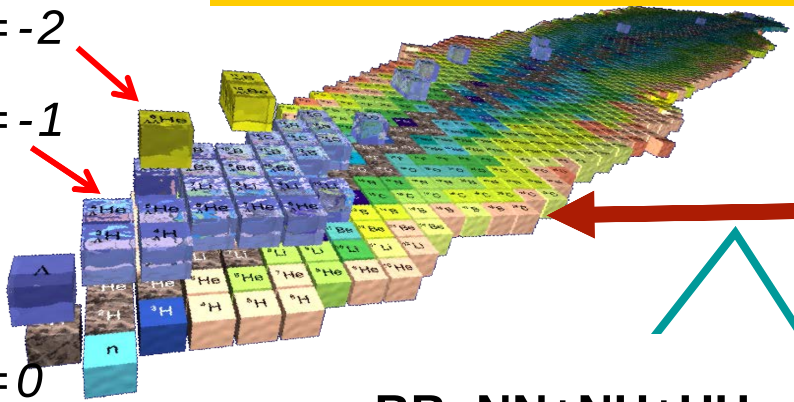

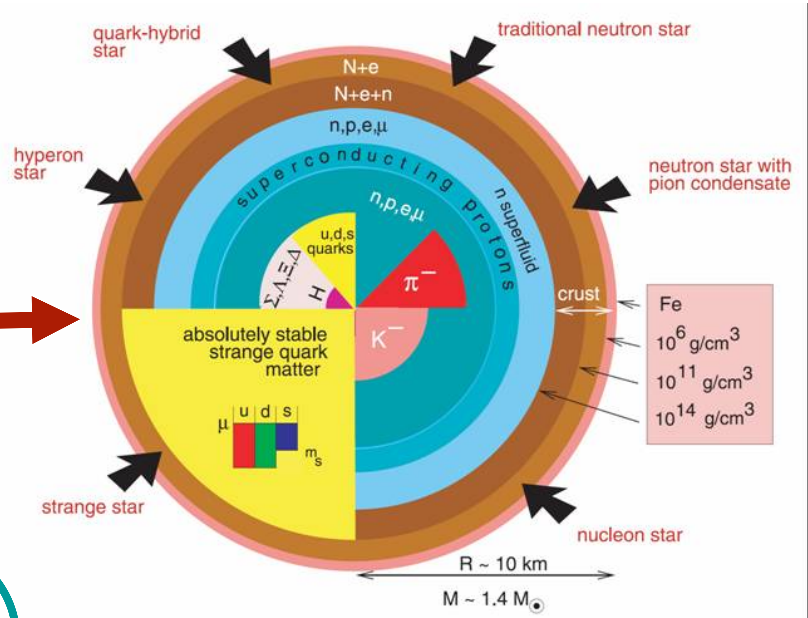

BB=NN+NH+HH

	n (udd)	P (uud)	Λ (uds)	Σ (uds)
n	N.R.	N.R.	S.H.	S.H.
p		N.R.	S.H.	S.H.
Λ			D.H.	D.H.
Σ				D.H.

The single and double hypernuclei are the main sources of the strange sector of baryon-baryon interaction

Hyperon Nucleon Interactions

YN	$B_\Lambda(^3{}_\Lambda H)$	$B_\Lambda(^4{}_\Lambda H)$	$B_\Lambda(^4{}_\Lambda H^*)$	$B_\Lambda(^4{}_\Lambda He)$	$B_\Lambda(^4{}_\Lambda He^*)$	$B_\Lambda(^5{}_\Lambda He)$
SC97d(S)	0.01	1.67	1.2	1.62	1.17	3.17
SC97e(S)	0.10	2.06	0.92	2.02	0.90	2.75
SC97f(S)	0.18	2.16	0.63	2.11	0.62	2.10
SC89(S)	0.37	2.55	Unbound	2.47	Unbound	0.35
Experiment	0.13 ± 0.05	2.04 ± 0.04	1.00 ± 0.04	2.39 ± 0.03	1.24 ± 0.04	3.12± 0.02

Accurate values of binding energies B_Λ of light hypernuclei is extremely important and needed for parameterization of the two body effective potential!!!

$$V_{\Lambda N}(r) = V_c(r) + V_s(r)(S_\Lambda * S_N) + V_\Lambda(r)(l_{\Lambda N} * S_\Lambda) + V_N(r)(l_{\Lambda N} * S_N) + V_T(r)S_{12}$$

High precision γ-spectroscopy has been successful for the spin dependent terms but unable to measure binding energies

Decay pion spectroscopy: a new era

New experimental program based on magnetic spectrometers was proposed: A. Margaryan et al. Jlab, LOI-07-001, 2006

Experiments started at Mainz, A. Esser et al., 2013; Patrick Achenbach, et al. 2017

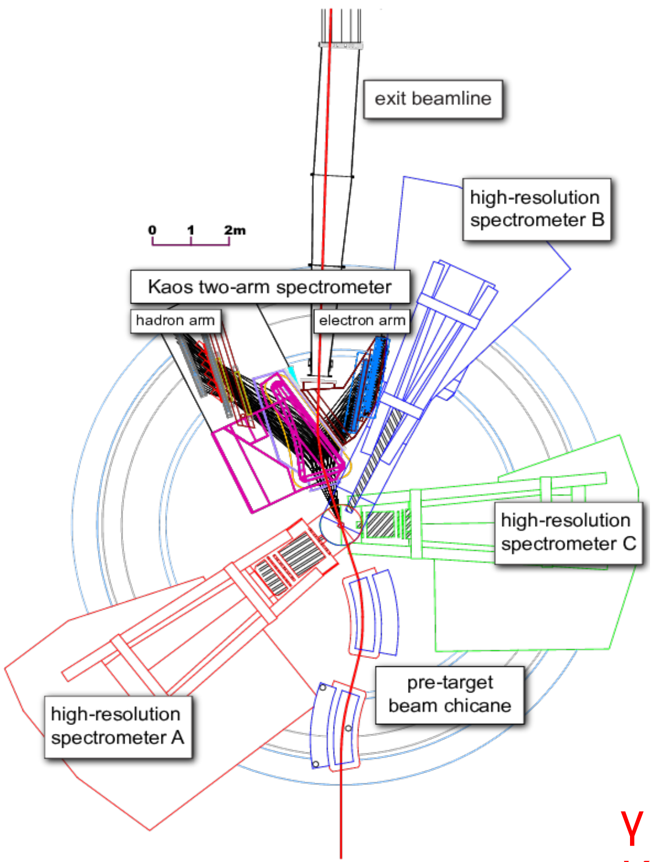

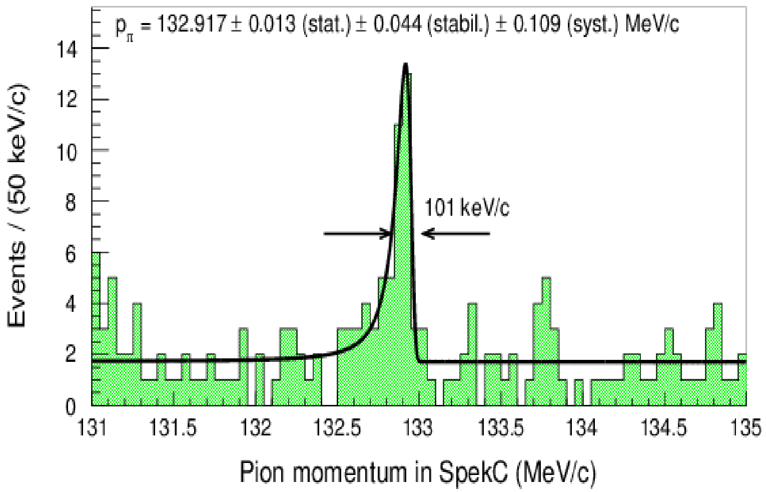

A monochromatic peak at 133 MeV/c was observed which is a unique signature for the two-body decay of 50 stopped hyperhydrogen ${}^4_\Lambda H \rightarrow {}^4He + \pi^-$ for a period of the two week beam time

γ + p → Λ + K⁺ reaction serve as a source of Λ and K^+ detection (eff. Is ~ 10^{-3}) used as a tag

Decay Pion Spectroscopy→Delayed Pion Spectroscopy

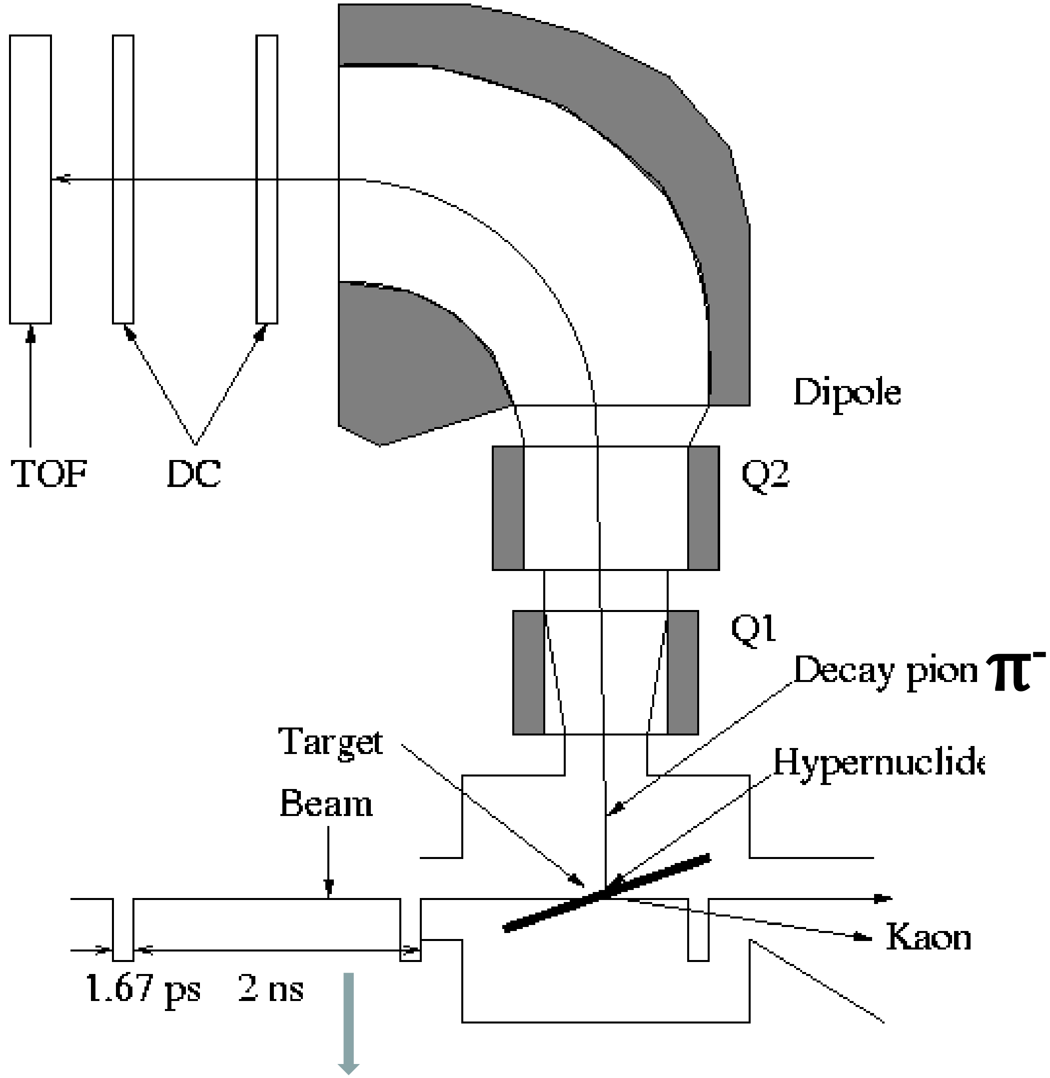

Hyperfragment lifetime is determined by weak interaction and is about 200 ps

A key of delayed pion spectroscopy is precision time measurement in the 100 ps range

Hyperfragment yield increased orders of magnitude

A. Margaryan et al. 2006; 2014.

Time structure of electron beams at Mainz and CEBAF
Ultra-precision time measurement allows delayed pion spectroscopy

Radio Frequency Time Measuring Technique (Streak Principle)

Streak Principle: convert time dependence of an optical signal to a spatial dependence of the accelerated photo-electron

Position Sensitive Detector

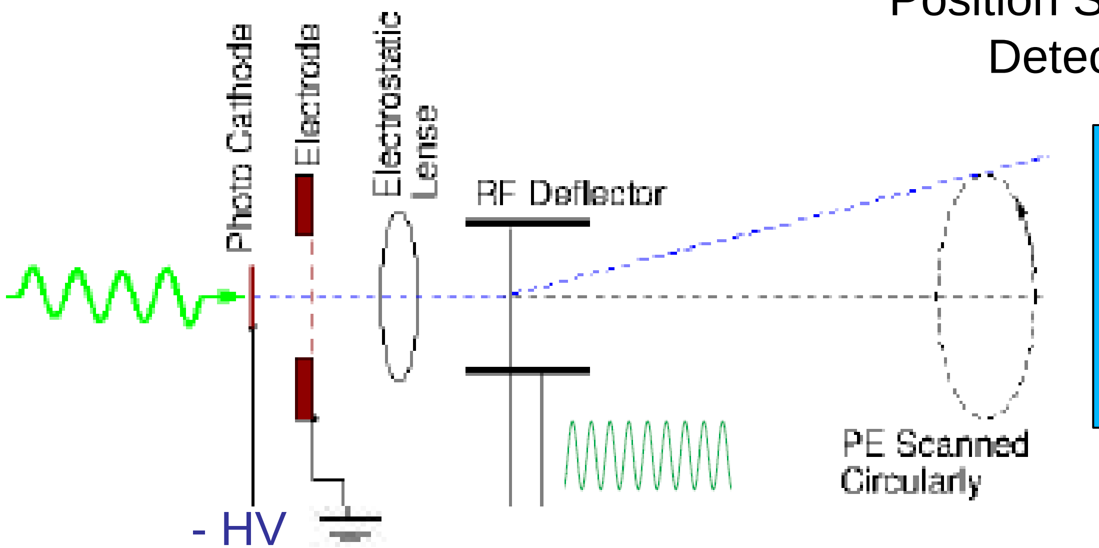

(X,Y) = Time

Image Readout
e.g. by using CCD

Schematic of the Streak Principle

Time resolution σ < 1 ps
Time stability stability - 200 fs/h
Time drift is ~10fs/s;
Image processing rate is ~few 10 kHz

see e.g. W. Uhring et al., Rev. Sci. Instr. V.74, 2003

Shamaev Helical RF Deflector

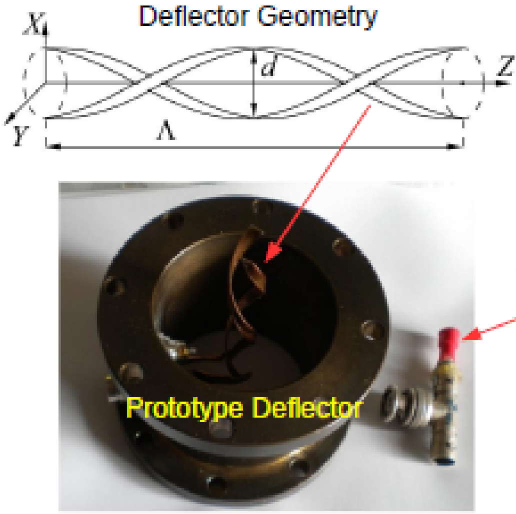

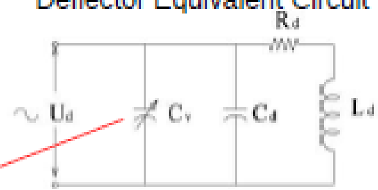

C_v tunes resonant behaviour to desired RF frequency

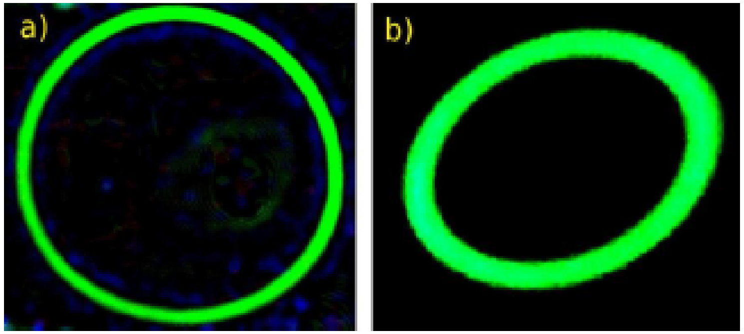

Deflected 2.5 keV electron beam @ phosphor screen.
Deflector: Λ=3 cm, d=1 cm, U_d=20 V,
U_a 2.5 kV, D=12 cm.
Applied RF frequencies (a) 1000 MHz; (b) 750 MHz.

- Helical electrodes: optimised to the velocity of the transiting electrons
- Loss of deflection sensitivity due to finite transit time effects is avoided.
- Electrodes form a resonant circuit, with Q > 100.
- On resonance, sensitivity of the deflection system ~1 mm/V or 0.1 rad/W$^{1/2}$
- ~1 W (into 50Ω) RF power sufficient to scan 2.5 keV electrons circularly 2 cm radius.
- Order of magnitude reduction in required RF power

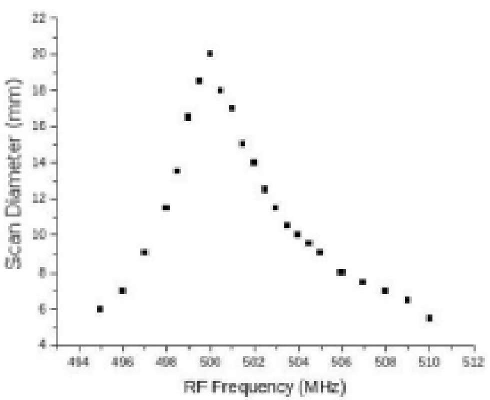

Diameter scanning circle vs RF frequency
500 MHz deflector. Λ = 6 cm, d = 1 cm,
U_d = 10 V, U_a = 2.5 kV, D = 12 cm.

The Radio Frequency Photomultiplier Tube

Principle of Operation

A. Margaryan et al., Nucl. Instr. and Meth. A 566, 321, 2006

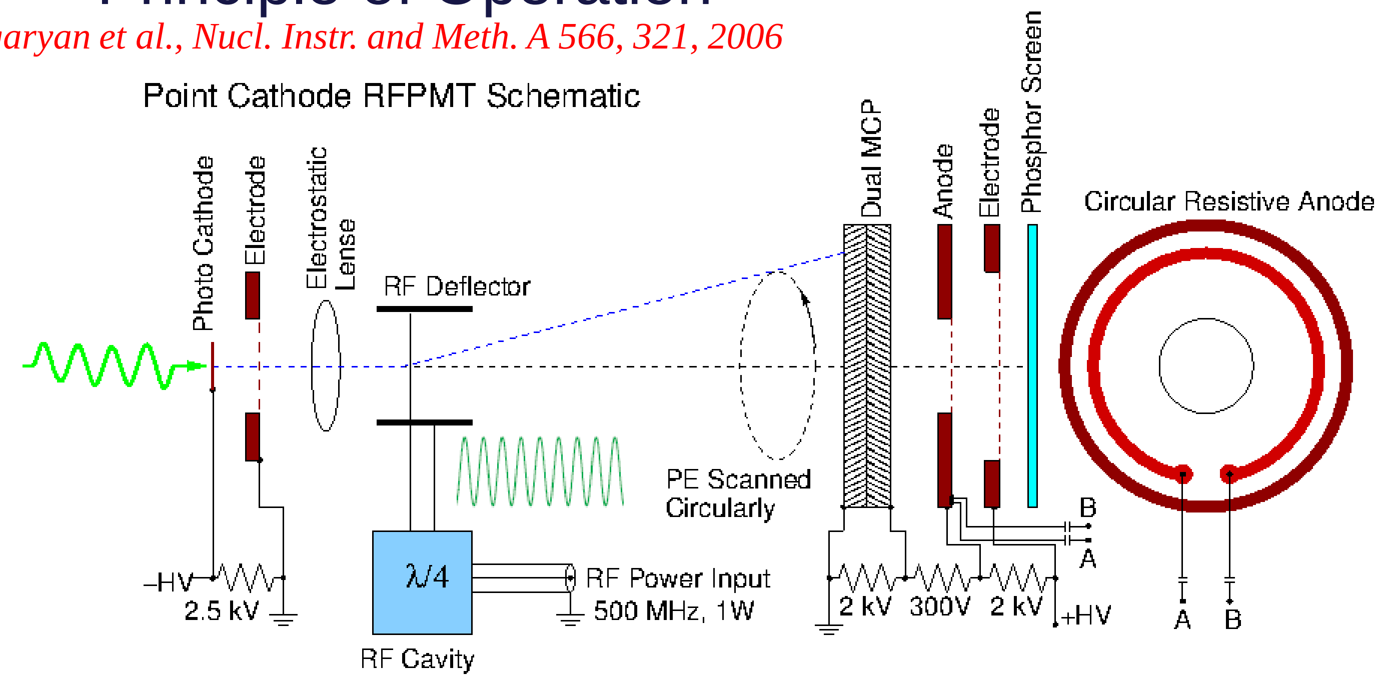

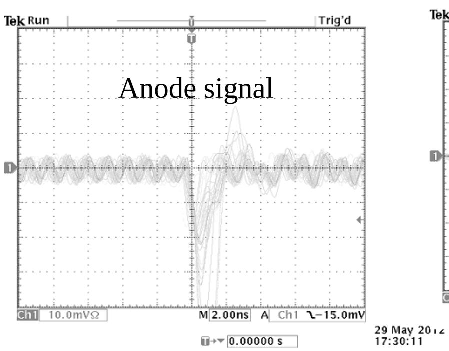

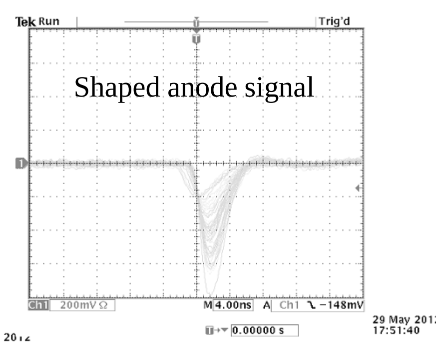

- Circular sweep RF deflection of photo electrons
- Convert time to spatial dependence
- Fast position sensitive electron detector
- MCP Gain ~10^7
- Single photon counting possible
- Prototype device resistive anode
- Fast ~ns output pulse

Projected Time Resolution

RFPMT time resolution.

$$\delta\tau_{RF} = (\delta\tau_{tt}^2 + \delta\tau_d^2)^{1/2}$$

- $\delta\tau_{tt}$ resulting from electron Transit Time Spread (TTS): from computer simulation using SIMION-8.
- $\delta\tau_d$ resulting from position dispersion of the PE detected at the anode.

  $\delta\tau_d = \delta r/v,\ v = 2\pi R/T$
- Position resolution δr convolution electron beam spot size after acceleration, focusing and RF deflection, and the intrinsic position resolution of the anode. T is the RF period (2ns) and R is the radius of the deflected electrons (20mm) δr ~ 0.1 mm $\delta\tau_d$ ~ 1.6 ps (500 MHz RF)

SIMION-8 Small Area Cathode

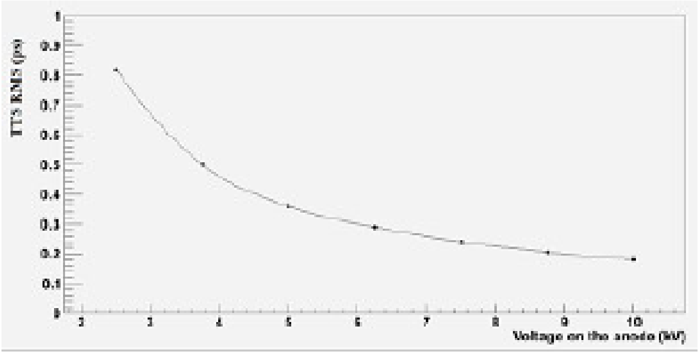

Simulations performed S. Zhamkochyan

SIMION-8 Extended Photo Cathode

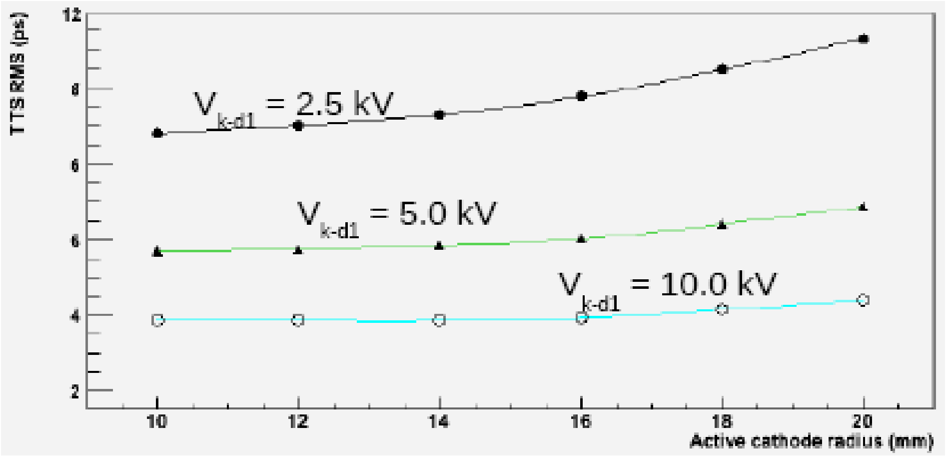

Mk1RFPMT produced by Photek, UK

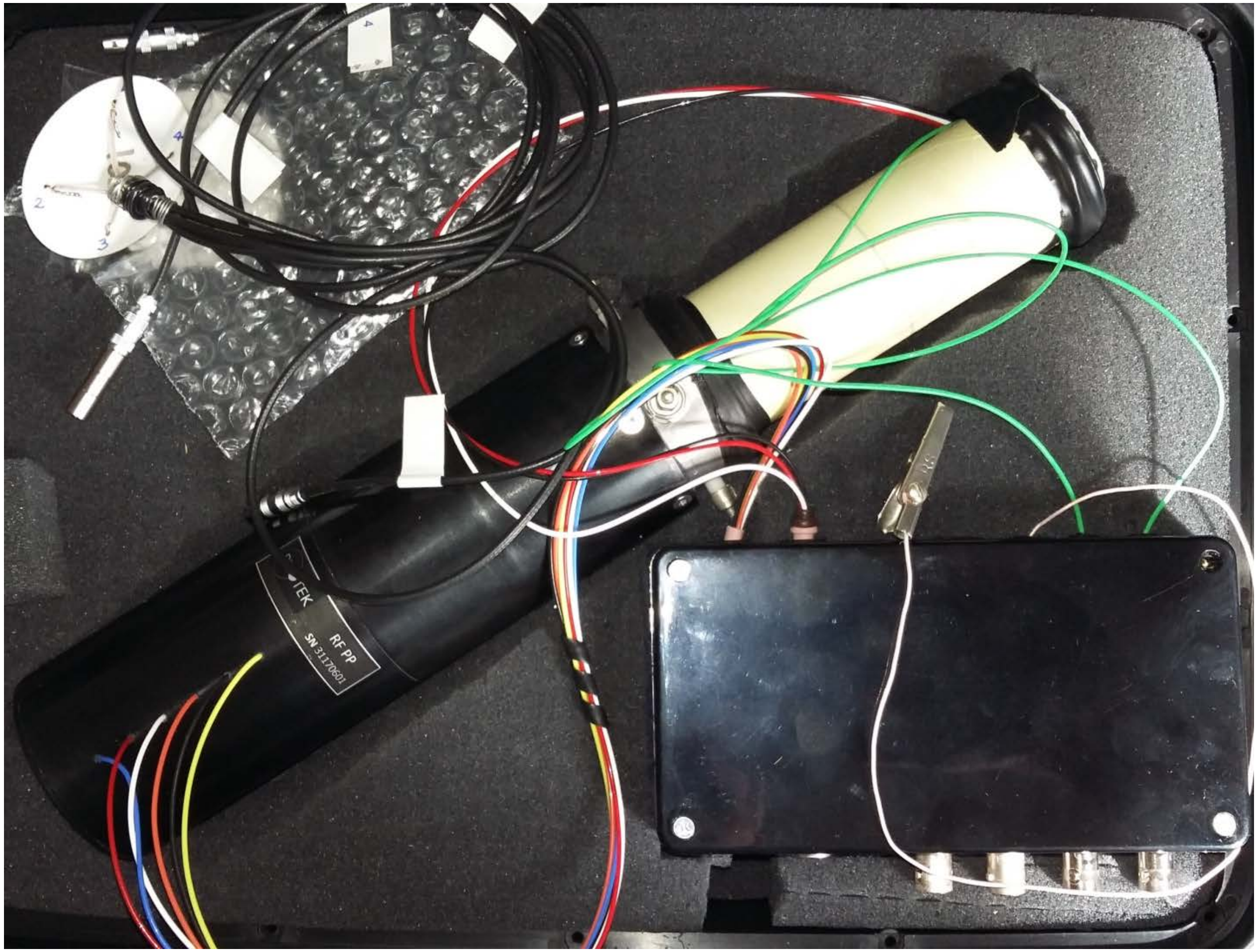

Test studies of the Mk1 RFPMT is continued at Alikhanyan Lab and CANDLE
Second prototype will be manufactured soon

RFPMT based high resolution single photon counting technique

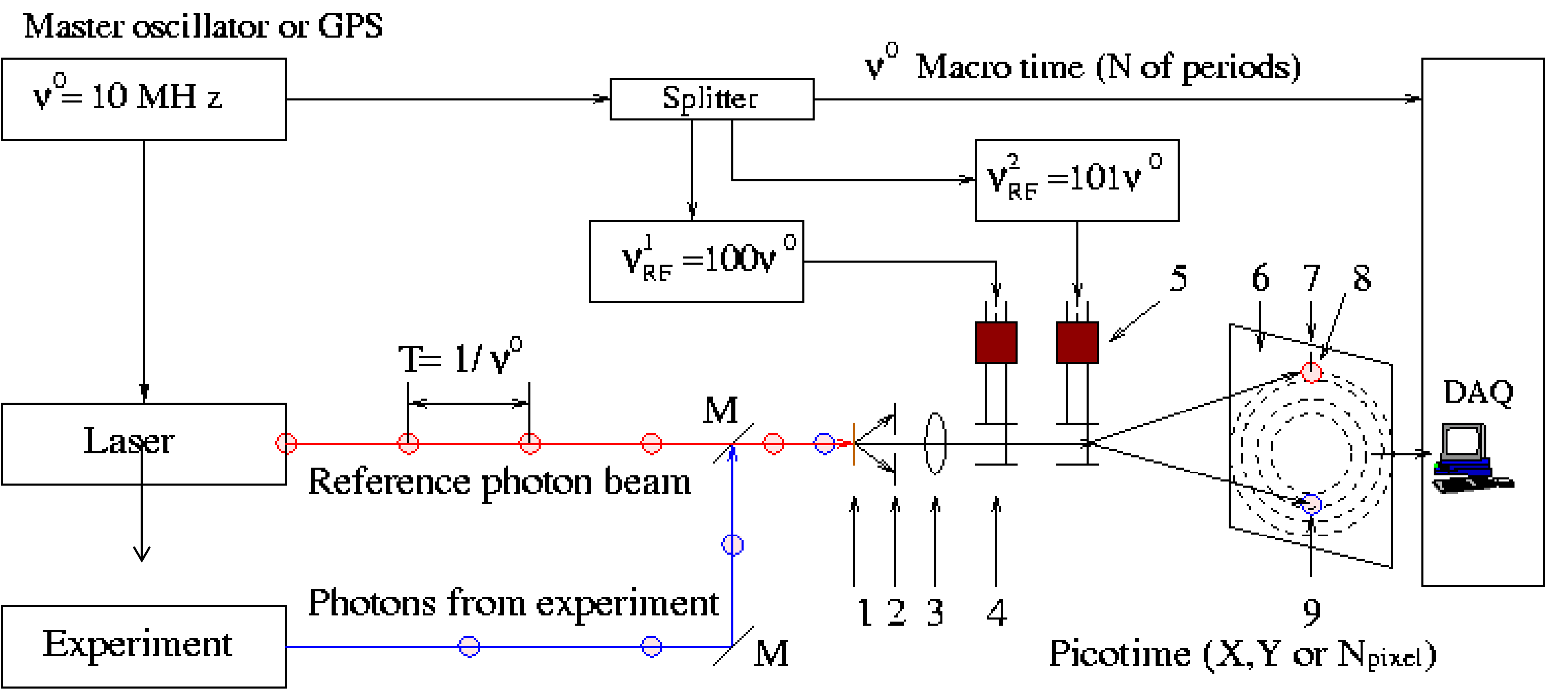

Schematic of the High Resolution (~1ps), Highly Stable (10 fs/h) and High Rate (> 1 MHz) Single Photon Counting Technique

A. Margaryan, 2010

Test studies will be carried out by using AREAL RF Synchronized laser beams

Calibration of the magnetic spectrometers with an accuracy $1{:}10^4$ by TOF measurement of pair of particles

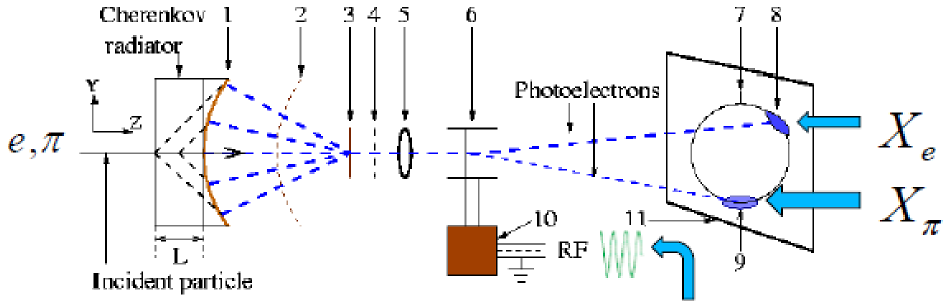

Synchron with the incident electron bunches

The Cherenkov Detector with the RF PMT

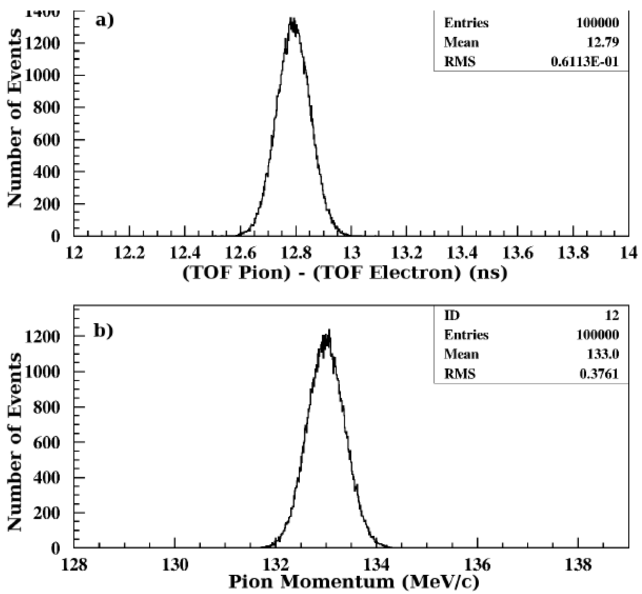

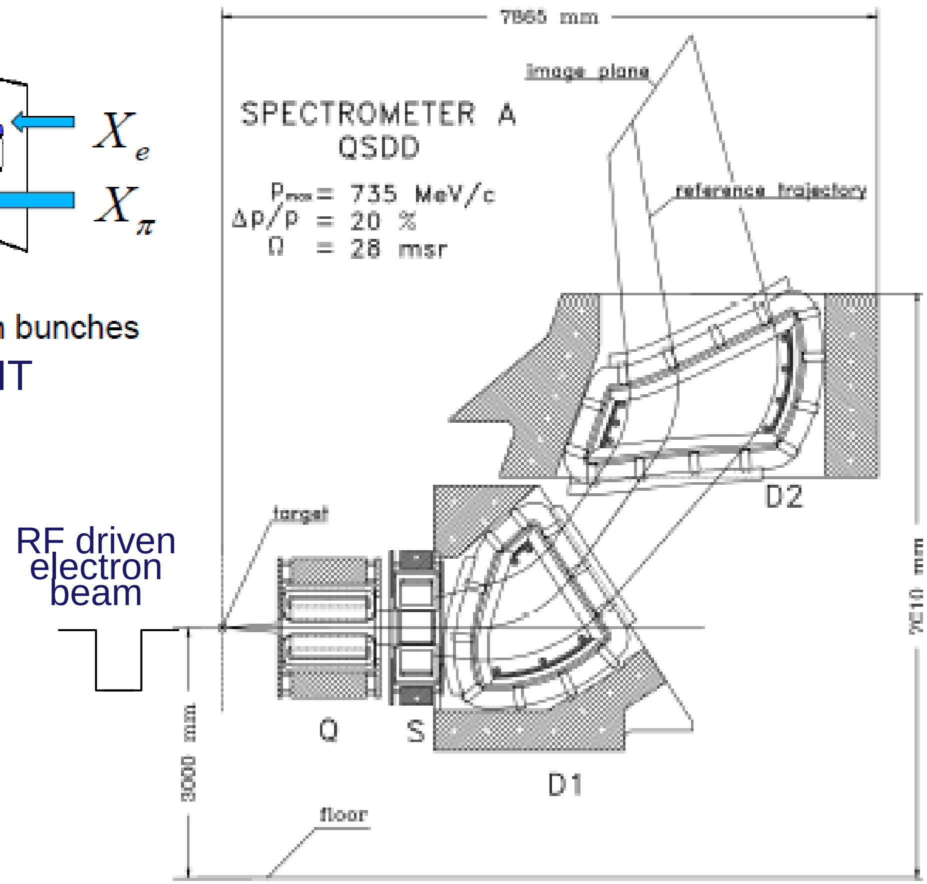

The SpekA at the Mainz Microtron MAMI

The distributions of the $t_\pi - t_e$ (a) and p (b). The mean values are:12791.4 ps and 133.00 MeV/c

A. Margaryan, J. Annand, P. Achenbach et al. Nucl. Instr. and Meth, 2016

Auger Neutron Spectroscopy of Λ Hypernuclei

The strong interaction of ΛN is a weak than NN interaction

Dominant decay of the excited states in the heavy hypernuclei is ejection of Auger neutrons (Likar, Rosina, Povh, Z. Phys. 1986).

A. Margaryan, et al.. Auger neutron spectroscopy of nuclear matter at CEBAF. Letter of intent to JLAB PAC 18, LOI-00-101 (2000).

C. Keil and H. Lenske. The hypernuclear Auger effect within the density dependent relativistic hadron field theory. Phys. Rev. C66, (2002)

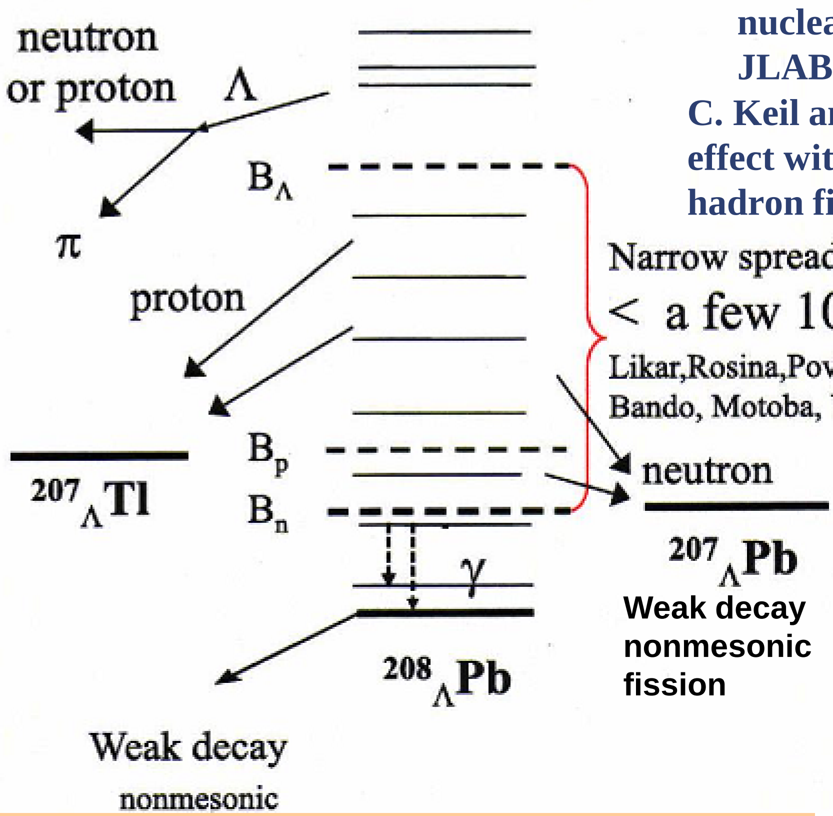

Heavy hypernuclear excited states and their decay Modes. Figure is taken from TJNAF Proposal E01-011

Auger neutron spectroscopy

Successful determination, with high energy resolution, of the 1s, 1d, 1f, 2p, 1g, 2d and 1h states in a heavy nucleus would truly be a major step in nuclear physics. PAC-18→LOI 00-101

Auger Neutron Spectroscopy: Experimental Approach

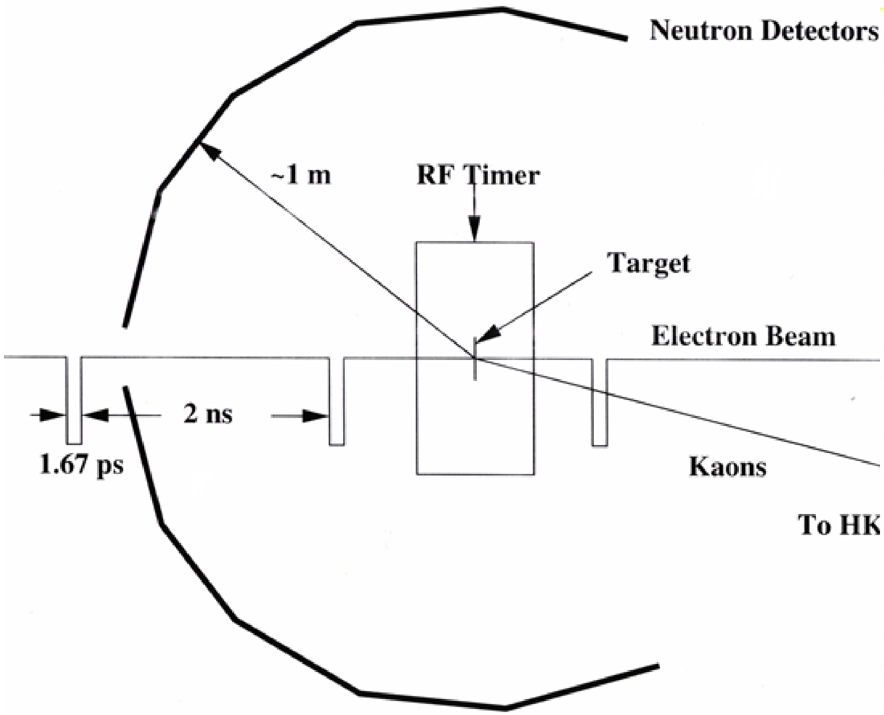

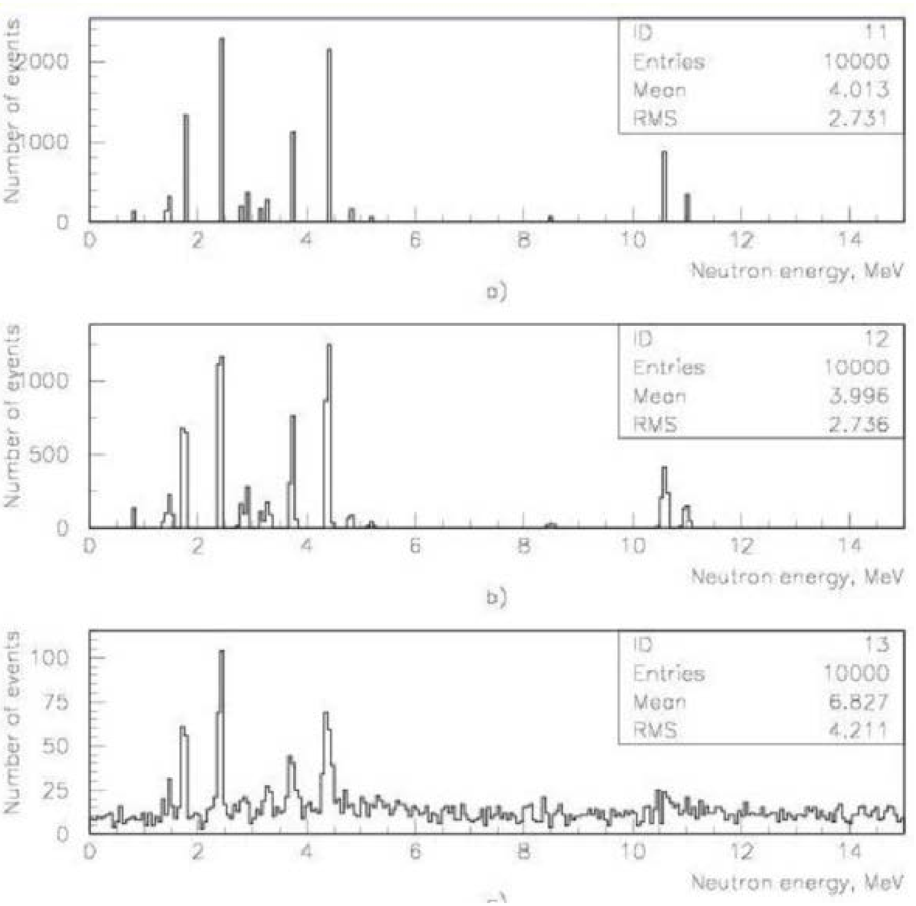

Schematic of the experimental setup

RF Timer is a RF time-zero fission fragment detector

Spectrum of the expected Auger transition strengths in $^{93}Nb_{\Lambda}$:
a) transitions in the c.m. system;
b) in the lab system with kinematical broadening;
c) in lab (700 AN+9.300 Background) energy resolution included.

The Radio Frequency Time-Zero Fission Fragment Detector

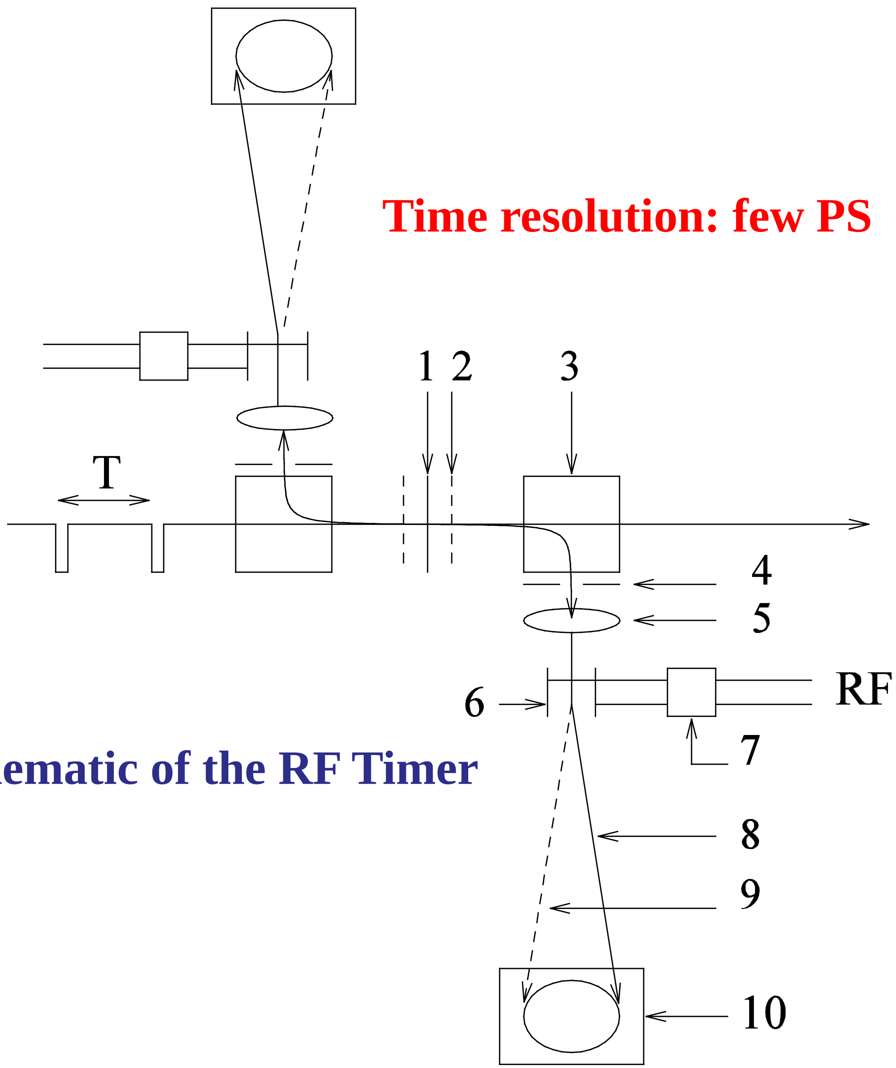

Time resolution: few PS

Schematic of the RF Timer

1. Target
2. Accelerating electrode
3. Magnet
4. Collimator
5. Electrostatic lens
6. RF deflector
7. RF matching system
8. Deflected prompt secondary electrons
9. Deflected delayed secondary electrons

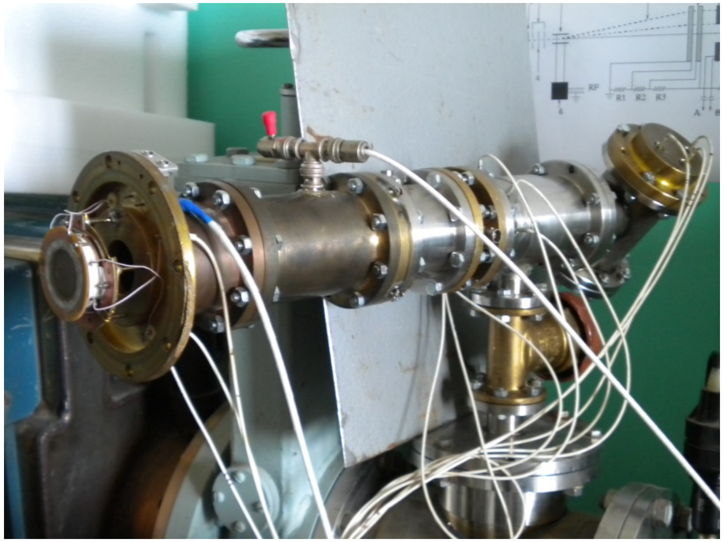

General view of the prototype detector

Prototype Detector will be ready soon
Test studies are planned at Alikhanyan Lab and Areal UV laser beam

Study of fissioning isomers at pulsed proton and photon beams

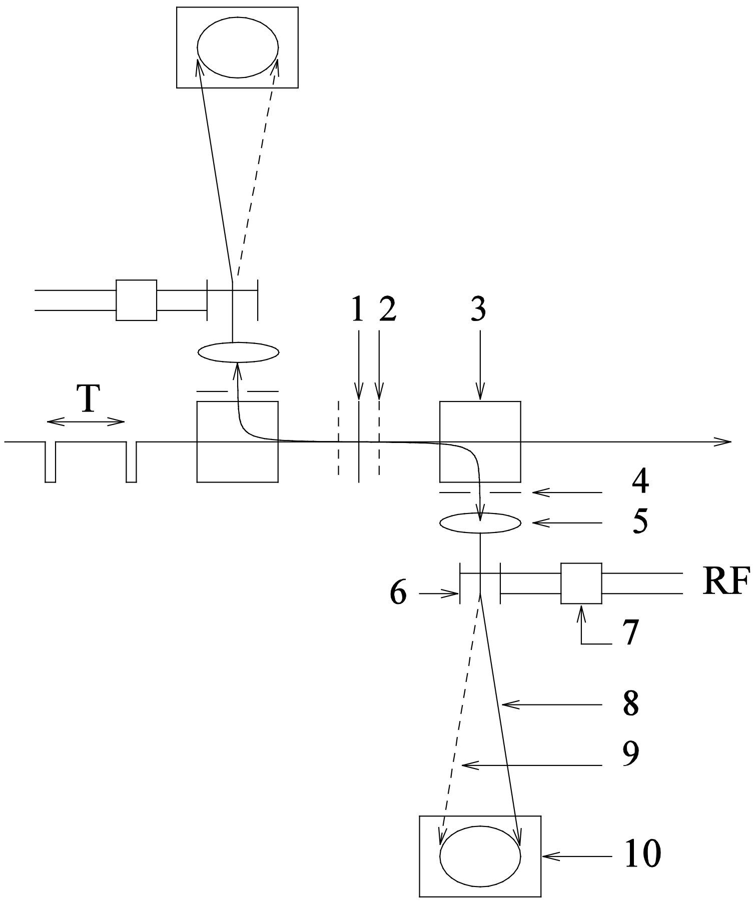

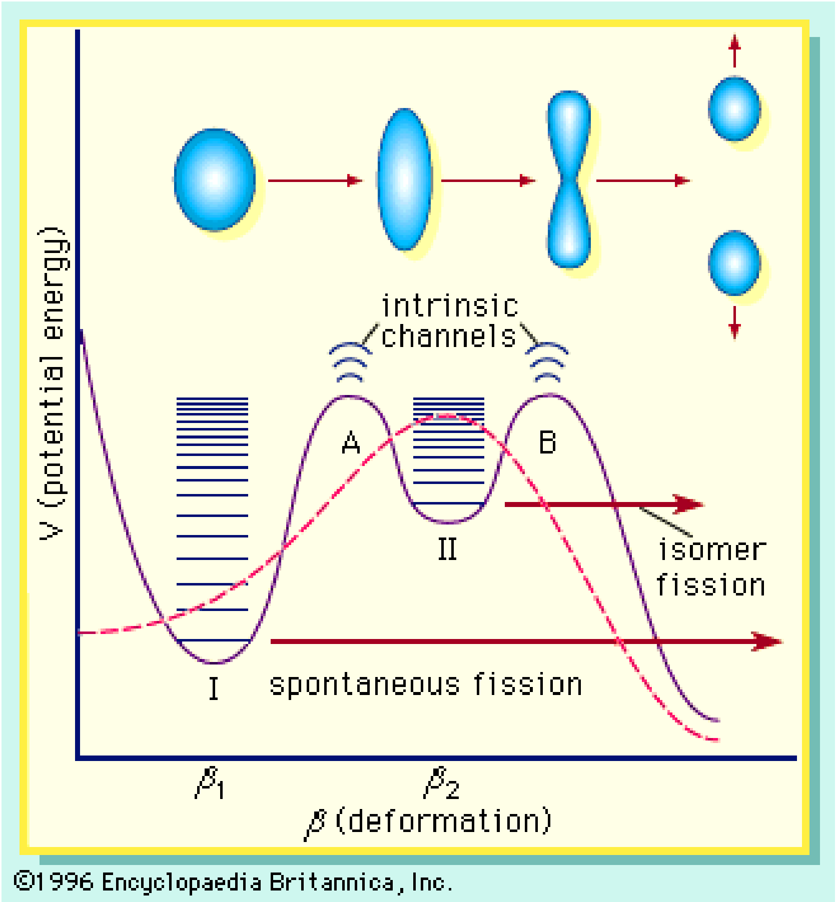

We are planning to study of the fissioning isomers with lifetimes laying in the range **10ps-10ns** at the pulsed proton (**Yerevan**) and photon (**ELI-NP)** beams

Helium Burning and the $^{12}C(\alpha,\gamma)^{16}O$ Reaction

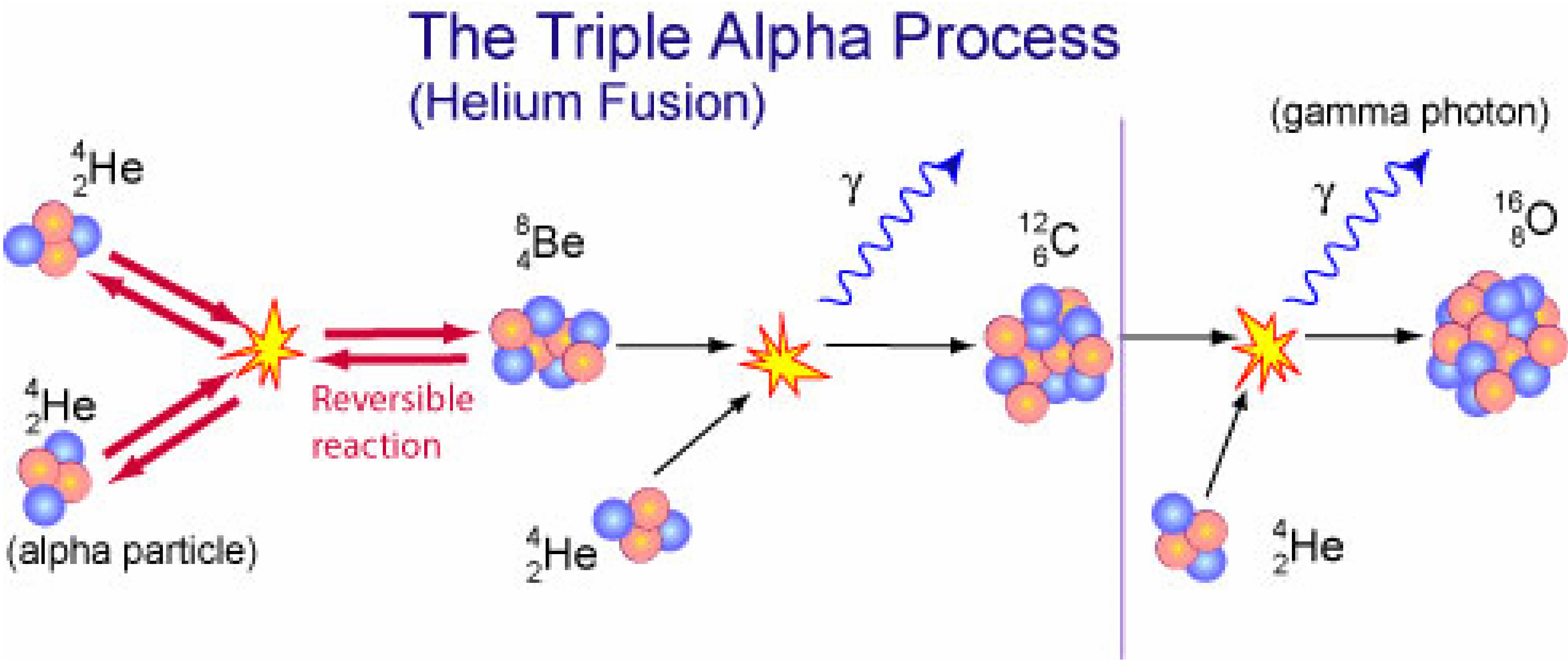

The triple alpha process plays crucial role in astrophysics!
The ratio of carbon-to-oxygen (C/O) at the end of helium burning is determined by the cross section of the $^{12}C(\alpha,\gamma)^{16}O$ reaction at the 300 keV, which is about 10^{-8}nb, i.e. non measurable in the Lab. One must measure at energies as low as possible and extrapolate to 300 keV.

The S-factor for the E1 component of the $^{12}C(\alpha,\gamma)^{16}O$ reaction

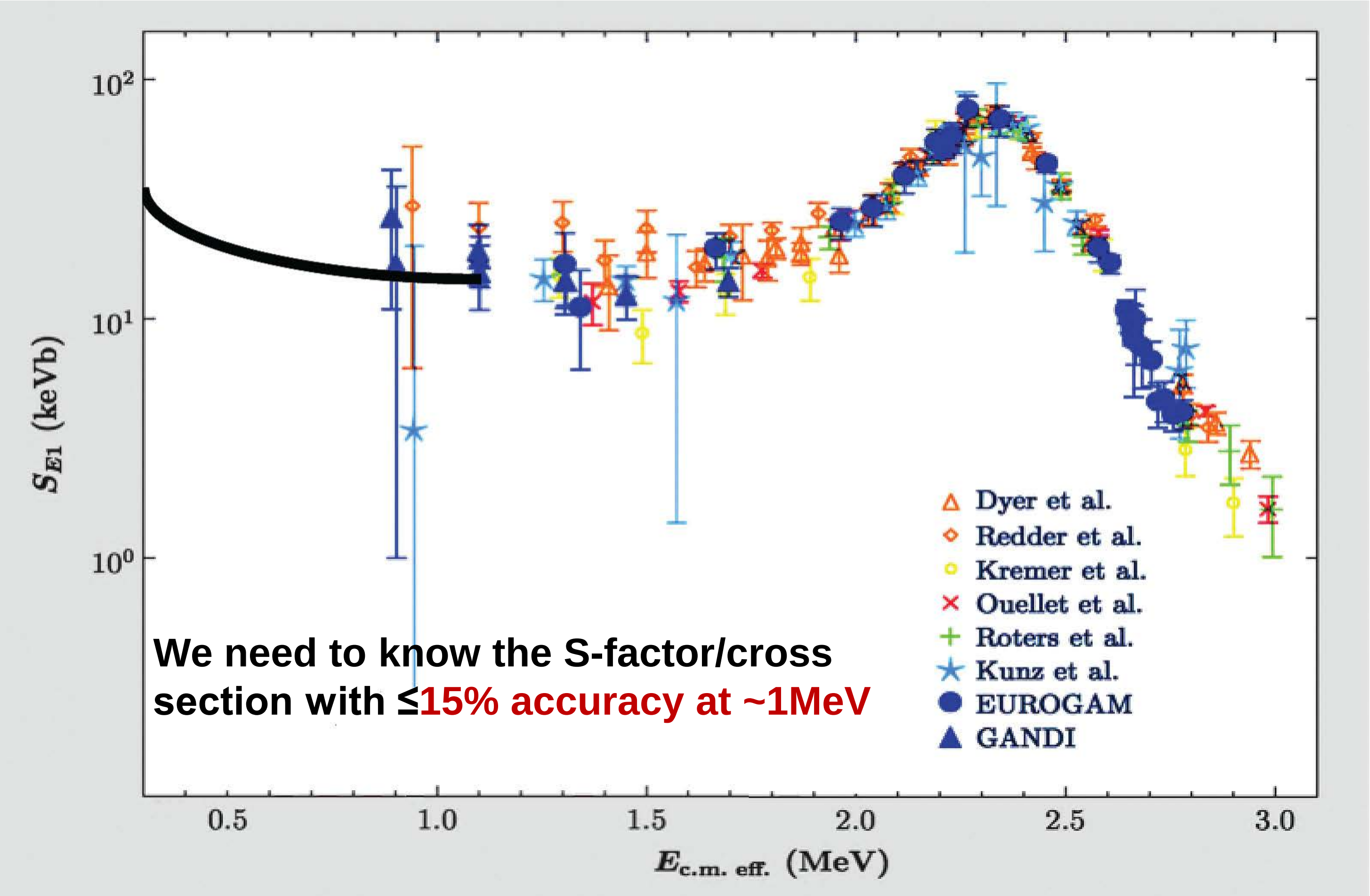

Data points correspond to some of the latest experimental direct measurement results. The solid line through the data represents **one of many possible extrapolations** into the astrophysically relevant energy region (~300 keV). Depicted from C. Ugalde et al., PR12-13-005

The $^{16}O(\gamma,\alpha)^{12}C$ reaction instead of $^{12}C(\alpha,\gamma)^{16}O$

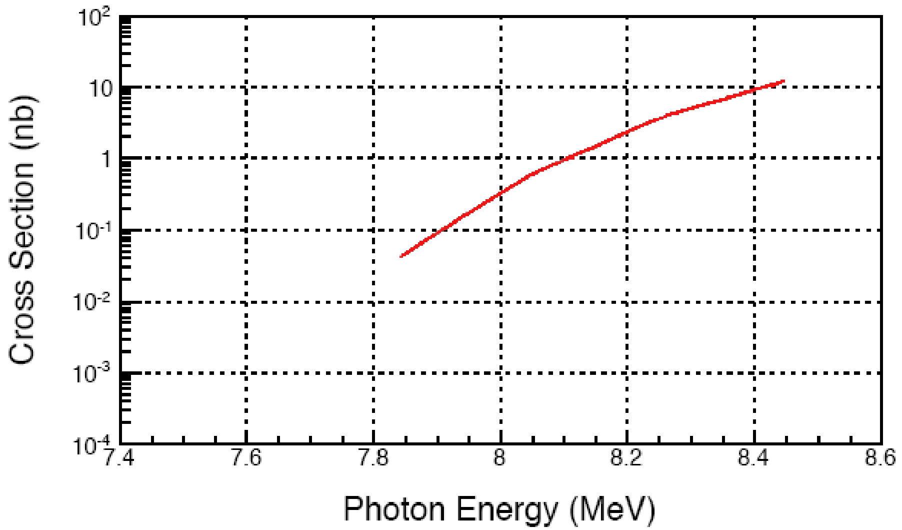

Principle of detailed balance

$$\omega_A \frac{\sigma_A(X,\gamma)}{\lambda_\alpha^2} = \omega_B \frac{\sigma_B(\gamma,X)}{\lambda_\beta^2}$$

1. **$\sigma(^{16}O(\gamma,\alpha)^{12}C) \approx 50\times\sigma(^{12}C(\alpha,\gamma)^{16}O) \approx$ 3 nb at $E\gamma \approx$ 8.2 MeV**
2. **Oxygen dissociation at $E\gamma$ = 8.2 MeV results ~0.750 MeV α particle and ~0.250 MeV ^{12}C**
3. **$\sigma(^{16}O(\gamma, e^+e^-)^{16}O) / \sigma(^{16}O(\gamma,\alpha)^{12}C) \approx 10^8$ at $E\gamma \approx$ 8.2 MeV**

Alpha Cluster Structure of Nuclei

Cluster structure of light nuclei is an other avenue which we are going to explore at Cyclon-18, ELI-NP and HIγS by using active targets

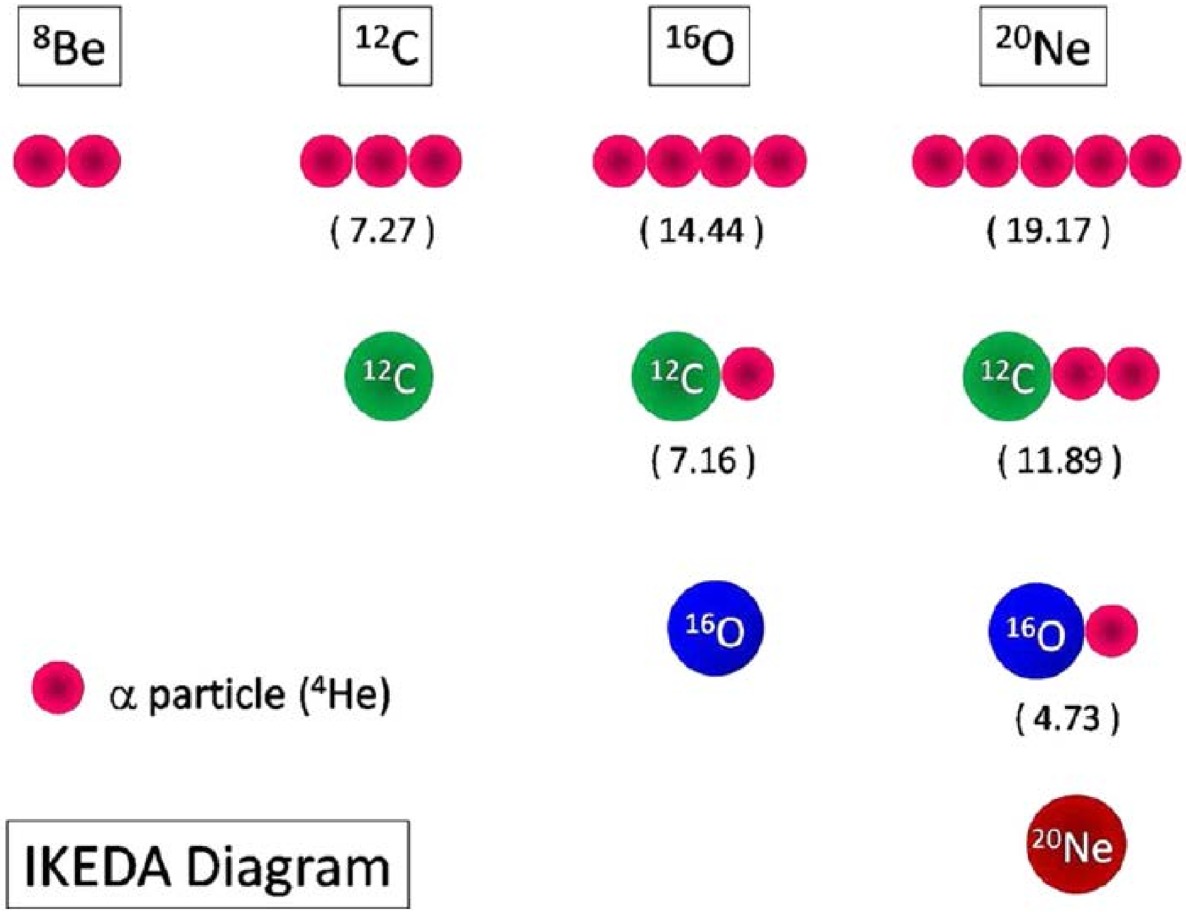

The so-called Ikeda diagram showing how above particle-breakup thresholds, the Structure of light alpha-conjugate nuclei can be thought of as comprised of alpha clusters

Low EneRgy Nuclear Interaction Chamber

Protons
20-300 keV
Deuterons
50-500 keV
Alpha
>50 keV
More heavy
Range
>30 mkg/cm^2

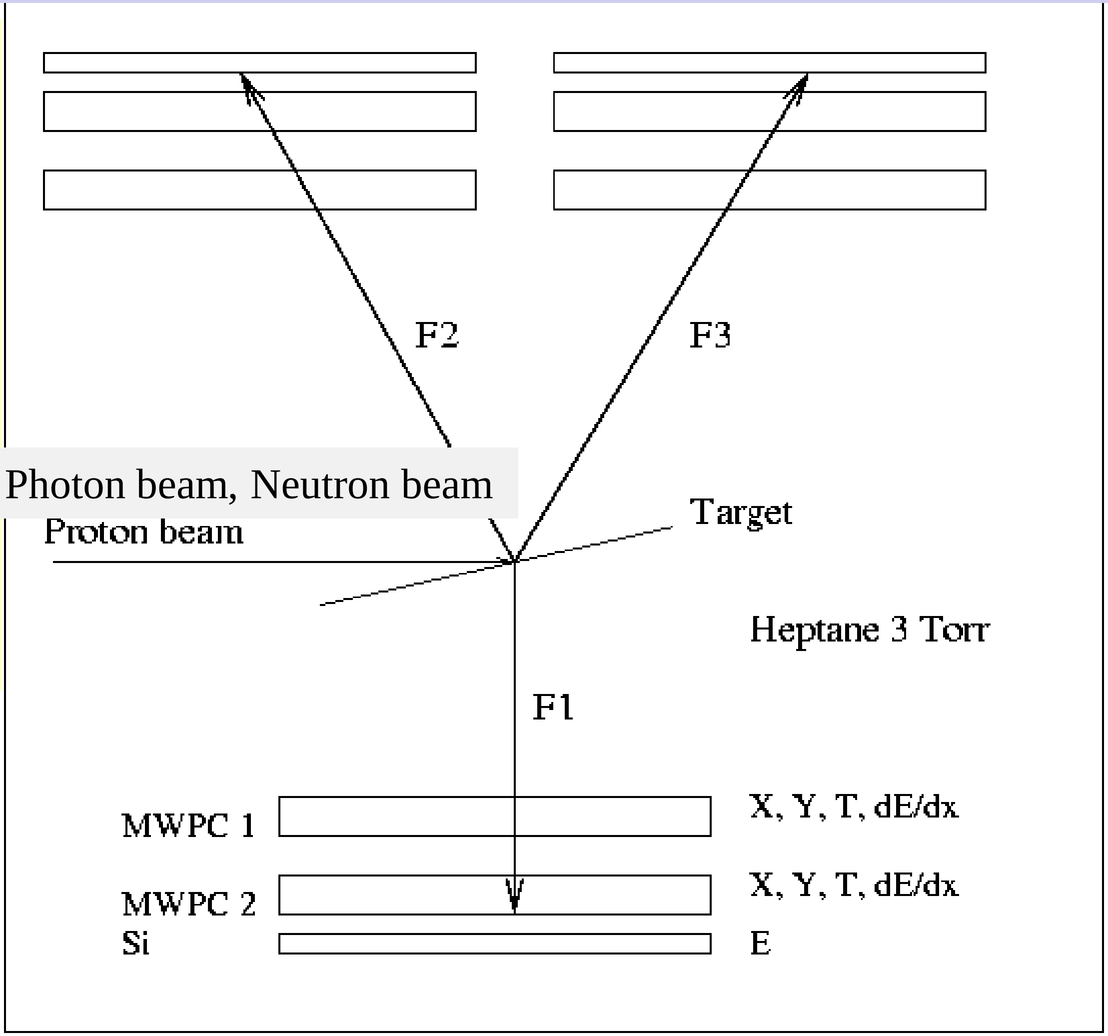

Schematic of the LERNIC

Targets
Working gas
H
D
He-3
He-4
$(OCH_3)_2CH_2$
C_6H_{14}
CF_4
Ne
Ar
Kr
Xe
And any thin foil from Mendelev table

General view of the prototype active target single arm and test setup

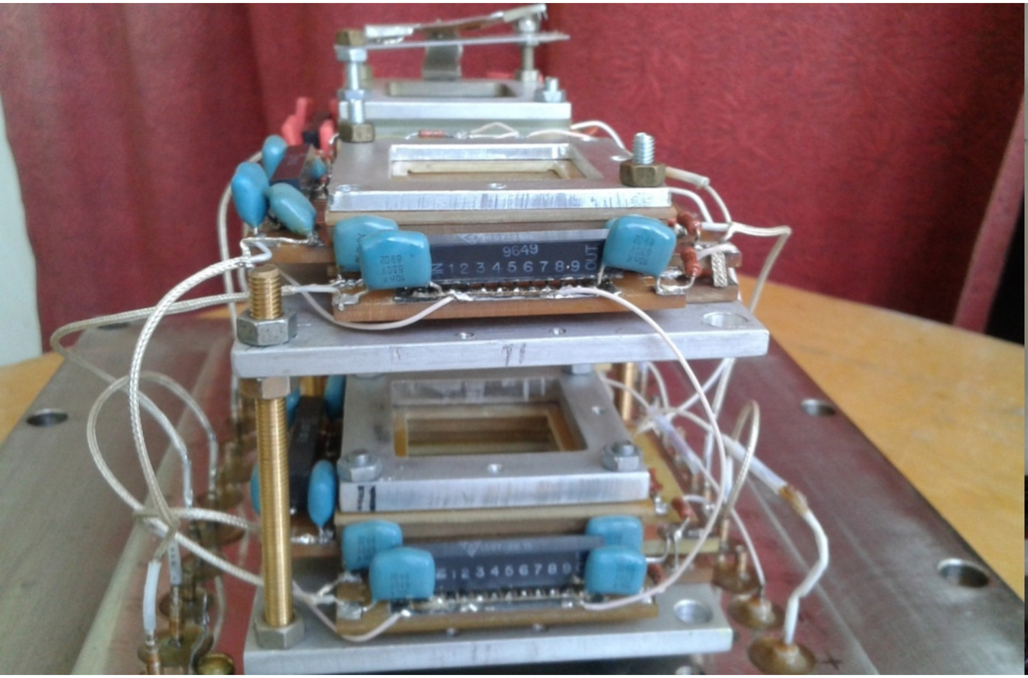

Single arm of the active target

General view of the test setup

Test studies in lab

Methyl ($(OCH_3)_2CH_2$) at 3-9 Torr

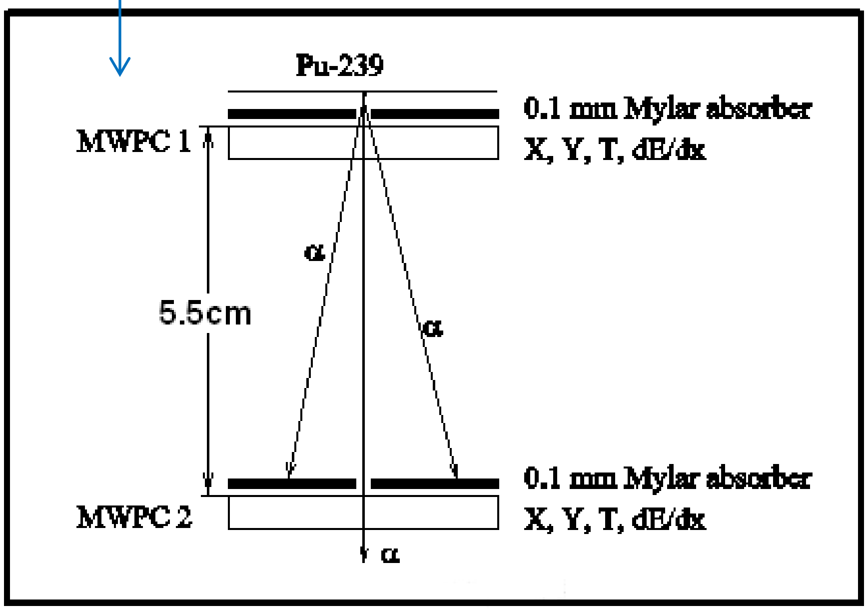

Schematic of the test setup
MWPC1 and MWPC2 are units of the windowless MWPC

Typical signals generated by α-particles:

a) directly from Pu-239 source,

b) after passing through 24 μm polyethylene

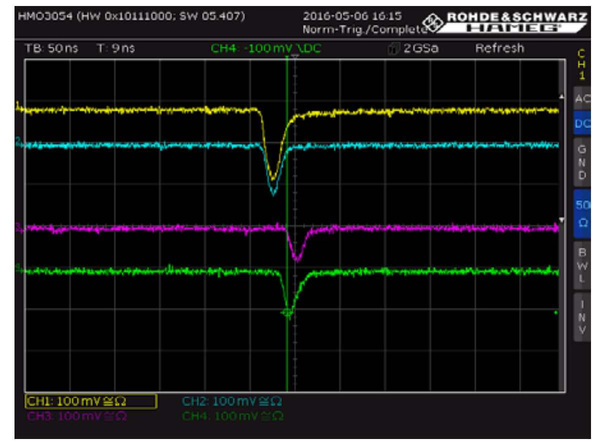

a)

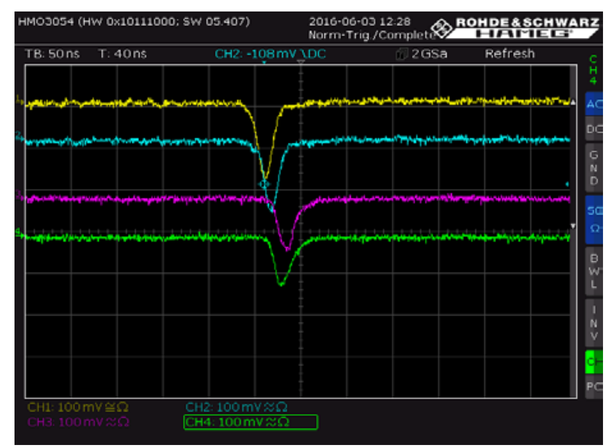

b)

Low-pressure MWPC test results

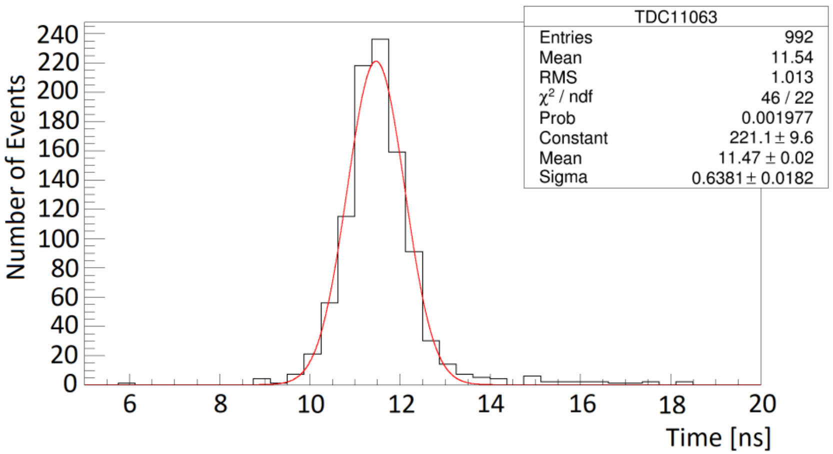

Time resolution

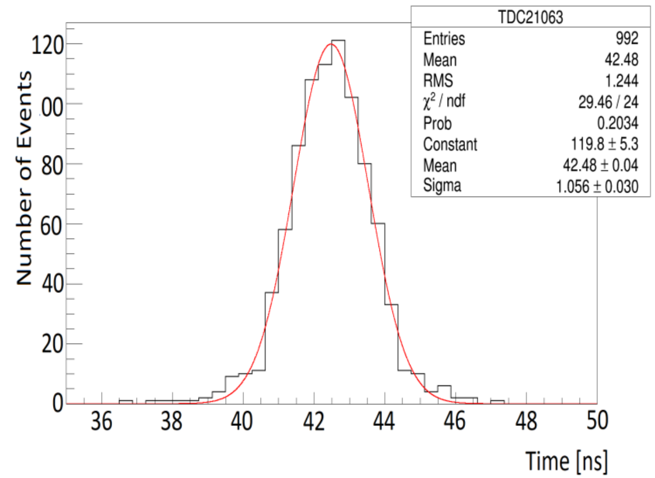

Position resolution

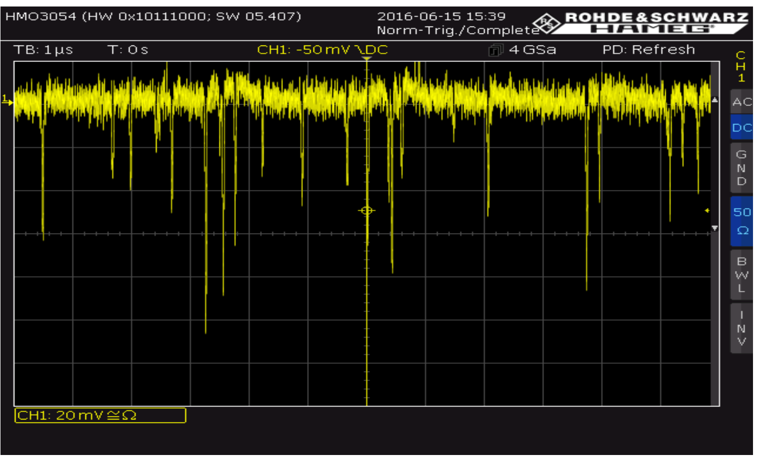

Rate capability

Summary of the test studies

1) Time resolution of the MWPC-≤ 450 ps
2) Position resolution of the MWPC ≤ 1.5 mm
3) Rate capability - few MHz
4) β-particle efficiency/α-particle efficiency ≤ 10^{-4}

Test Studies are planned at AREAL with a presence of the electron beam

The $^{16}O(\gamma,\alpha)^{12}C$ experiment at HIγS

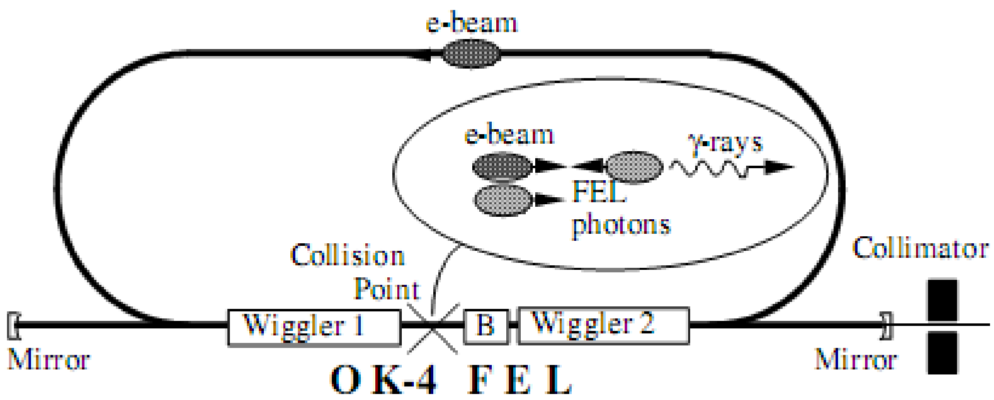

Schematic diagram of the HIγS facility

O-16 active target based on the low-pressure MWPC technique:
Advantages: ideal for detection of low-energy nuclear fragments, insensitivity to the electromagnetic background
Disadvantages: small number of target nuclei

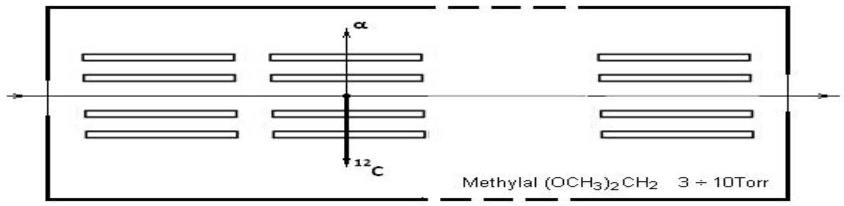

Schematic of the multi-module active target

Mode of HIγS operation: High-flux, quasi-CW operation

Angular Divergence $\Delta\theta \leq 0.2$ mrad

Collimated Flux ($\Delta E\gamma / E\gamma$ = 5% FWHM) = 2.4×10^8 photon/s at $E\gamma \leq 11$ MeV

Photon Beam bunch-length ≤ 200 ps

Photon Beam diameter ≤ 10.5 mm

Outlook

RF driven electron accelerators provide ultrafast, picosecond and sub-picosecond duration electron-photon pulses

We have developed principles of a 3H RF timing technique for single photons

- High resolution, 1 ps for single photon (limit 0.1 ps)
- High rate, few MHz → THz (is a realistic goal)
- Highly stable, ps/day→10 fs/day (synchronized with optical clock)

Combination of these two technologies opens new possibilities for nuclear and hypernuclear studies

We are planning to use the AREAL RF synchronized photon and electron beams for test studies of the RF Time-Zero Fission Fragment Detectors, RF PMTS and RFPMT based Cherenkov detectors.

The AREAL electron beam can be used also to reproduce the experimental conditions which are expected at high energy accelerators (Jlab, MAMI, HIγS, ELI-NP) which can serve as a cheap test lab for different type of detectors, e.g. for low-pressure MWPC based active targets.

Contributors & Collaborators

S. Abrahamyan, R. Ajvazyan, G. Ajvazyan, N. Grigoryan, H. Elbakyan, V. Kakoyan, P. Khachatryan, V. Khachatryan, S. Maylyan, H. Vardanyan, S. Zhamkochyan

Alikhanyan National Science Laboratory, 2 Alikhanyan Bros. Str. Yerevan 0036, Armenia

B. Grigoryan, A. Vardanyan

Center for the Advanced of Natural Discoveries using Light Emission, Yerevan, Armenia

J. Annand, K. Livingston, R. Montgomery

School of Physics & Astronomy, University of Glasgow, Scotland G128QQ, UK

D. Balabanski, C. Matei, D. Lattuada

ELI-NP, Magurele, Bucharest 077125, Romania

P. Achenbach, J. Pochodzalla

Institut fur Kernphysik, Johannes Gutenberg-Universitat, 55099 Mainz, Germany

S. N. Nakamura, S. Nagao, Y. Toyama

Department of Physics, Tohoku University, Sendai 980-8578, Japan

V. Sharry, D. Yvon

CEA-CE Saclay, France

I. Filikhin, B. Vlahovic

Department Science and Technology, North Carolina Central University, Durham 27707, NC, USA

Michael Wiescher, Richard James DeBoer

University of Notre Dame, Notre Dame, 46556, IN, USA

Acknowledgement: This work was supported by the Committee of Science, Armenia and ARPA Institute, USA, in the frames of the research projects 15T-2B206 and 18Ap_2b05, the International Science and Technology Center (ISTC, Kazakhstan) grant A-2390.

Thanks for your attention